DRIVEN PILE CAPACITY IN CLAY AND DRILLED SHAFT CAPACITY IN ROCK FROM FIELD LOAD TESTS

Yasser A. Hegazy, Ph.D., P.E.
D'Appolonia Engineering
Monroeville, PA-USA-15146

Andrew G. Cushing, E.I.T.
D'Appolonia Engineering
Monroeville, PA-USA-15146

Christopher J. Lewis, P.E.
D'Appolonia Engineering
Monroeville, PA-USA-15146

ABSTRACT

In this study, two case histories of deep foundations are discussed, including driven piles and drilled shafts. The first case history is an assessment of driven pile capacity in clay. As part of selecting the deep foundation system, steel pipe, concrete, and timber piles were driven at the site. Static compression and uplift load tests were performed on the concrete and timber piles, while only static compression tests were performed on the steel pipe piles. Measured pile capacities from the static load tests were compared to predicted pile capacities, which were obtained from empirical design methods employing laboratory and in-situ test results. The data demonstrate that the traditional alpha method results in somewhat conservative predictions for the test piles, regardless of whether the values of undrained shear strength (s_u) are obtained directly from the unconfined compression (UC) test or are inferred from a correlation with the CPTU as equivalent direct simple shear (DSS) values of s_u.

The second case study involves an evaluation of the axial and lateral capacities of drilled shafts in rock to support a concrete gated dam. The test drilled shafts were step-tapered from 5.5-ft diameter through the soil zone to 5-ft diameter in the rock socket. Axial and lateral load tests were performed on drilled shafts embedded in soft to medium hard clayey shale and claystone overlain by granular alluvium. The data demonstrate that longstanding methods of determining ultimate side resistance are conservative relative to the measured values, as are customary presumptive values, but that predictions using one evolving method can be unconservative in the absence of field verification. In addition, the shafts performed satisfactorily under the applied design load, exhibiting minimal lateral deflection within the rock socket.

INTRODUCTION

This paper presents two case histories of deep foundation installation and load testing. The first involves pipe, timber, and concrete piles driven into clay, and tested in axial uplift and compression, in association with the expansion of an industrial facility located near the Mississippi River in Louisiana. The second involves axial and lateral load testing of rock-socketed drilled shafts for the new Braddock Gated Dam on the Monongahela River near Pittsburgh, Pennsylvania. The details of pile and shaft geometry, soil and rock stratigraphy, and load-displacement are provided. In addition, the measured results are discussed in the context of existing predictive methodologies.

DRIVEN PILE FOUNDATIONS FOR INDUSTRIAL PLANT, LOUISIANA

The first case history documents the subsurface exploration and pile load test program associated with a proposed industrial facility in Louisiana. The 33-acre parcel is bounded by the Mississippi River approximately two miles to the west, and is 19 ft above mean sea level, on average.

Geotechnical Conditions

The subsurface stratigraphy consists of deltaic clays and silts, to a depth of about 140 ft, which overlie the regional fresh water Gonzalez Aquifer. The upper 10 to 12 ft of soil consists of a stiff to very stiff low plasticity clay and silty clay, which is heavily overconsolidated due to desiccation. This soil is underlain by a stiff to very stiff, moderately overconsolidated, highly plastic clay to silty clay layer to a depth of about 50 to 70 ft.

Undrained shear strength measurements were obtained using the laboratory unconfined compression (UC) test and field vane shear test (VST), as depicted in Figs. 1 and 2, respectively. Mean values of laboratory s_u(UC) and peak field s_u(VST), corrected for plasticity index (Bjerrum, 1972), equal 1375 psf and 3300 psf, respectively.

Cone penetration tests with porewater measurements (CPTU) were also performed at the site. The soil undrained shear
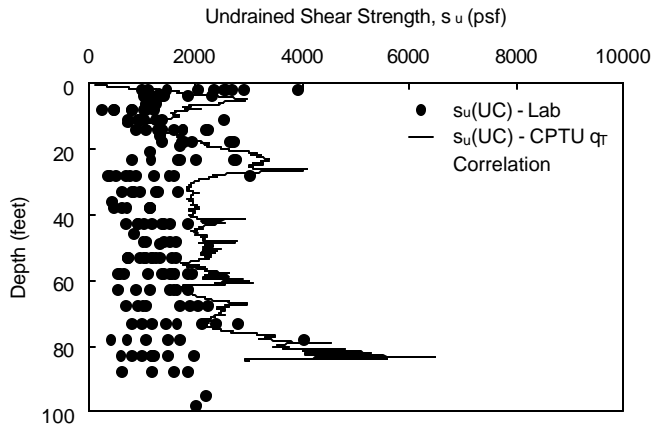
Fig. 1. Variation in laboratory values of $s_u(UC)$ with depth, compared to inferred $s_u(UC)$ profile from CPTU q_T
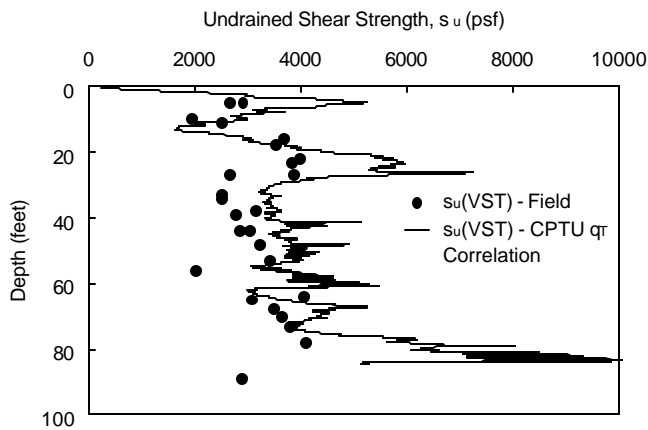

Fig. 2. Variation in peak field values of $s_u(VST)$ with depth, compared to inferred $s_u(VST)$ profile from CPTU q_T

strength was also estimated as a function of corrected cone tip resistance (q_T) and total overburden stress (σ_{vo}), as follows (Kulhawy, et al., 1992):

$$s_u(UC) = 0.0512 \, [q_T - \sigma_{vo}] \tag{1}$$
$$s_u(VST) = 0.0906 \, [q_T - \sigma_{vo}] \tag{2}$$

Equations 1 and 2 were employed using mean values of q_T from 16 CPTU tests conducted at the site to develop inferred $s_u(UC)$ and $s_u(VST)$ profiles, which are shown on Figs. 1 and 2, respectively.

An evaluation of the data in Fig. 2 demonstrates that Eqn. 2 provides reasonable estimates of peak field $s_u(VST)$. This observation can be explained by the fact that both the VST and CPTU tests maintain, to a reasonable degree, the in-situ soil stress state, which directly influences soil strength.

Consideration of the data in Fig. 1, however, demonstrates that nearly all of the laboratory-measured values of $s_u(UC)$ are less than the $s_u(UC)$ profile inferred from CPTU q_T data. In fact, averaging the laboratory $s_u(UC)$ data over the driven pile

lengths at the site yield soil strength values which are on the order of 60% to 65% of the average $s_u(UC)$ profile values inferred from the correlation with CPTU q_T. This discrepancy can partly be attributed to the influences of soil anisotropy, in addition to the stress relief and sample disturbance that soil specimens experience before being tested in unconfined compression (Ladd and Foott, 1974).

Steel Pipe Piles – Static Compression

Four steel pipe piles were initially driven at the site to a depth of 52.5-ft, with an additional 1-ft restrike four days later. Each test pile consisted of a 14-inch outside diameter steel pipe ($f_y = 45$ ksi) with 0.281-inch wall thickness, with closed ends consisting of ¾-inch thick steel plates welded flush with the outside diameter. A Vulcan 06 air hammer was used, and the driving record for each pile is provided in Fig. 3. Pile penetration rates at the end of initial installation ranged from approximately 20 to 30 blows/ft, and increased to 40 to 83 blows/ft for the 1-ft restrike. Each pile was subsequently load tested in accordance with ASTM D 1143 ("Standard Test Method for Piles Under Static Axial Compressive Load"). Load-displacement curves for the static compression load tests on the steel pipe piles are provided in Fig. 4.
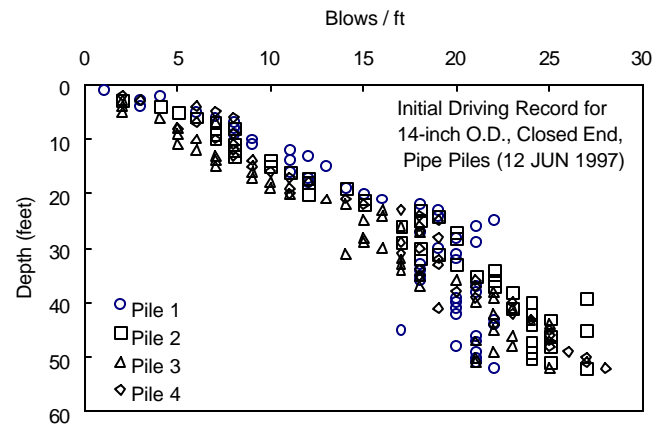

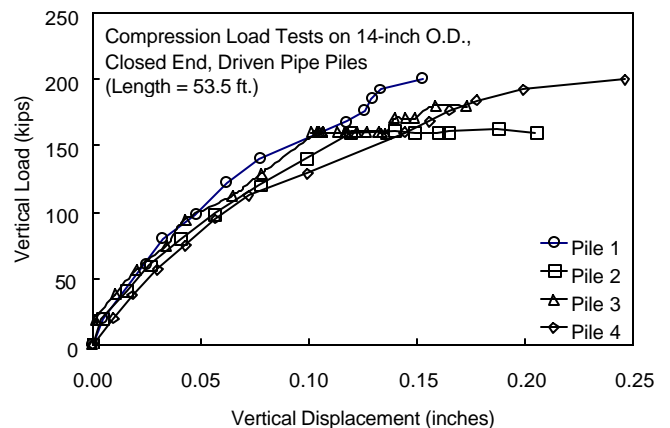*Fig. 3. Initial driving records for 14-inch O.D. pipe piles*

Fig. 4. Load-displacement curves for axial compression load tests on 14-inch O.D., closed end, driven pipe piles

Concrete and Timber Piles – Static Compression and Uplift

Concrete and timber piles were also driven at the site and statically load tested in both compression and uplift. The concrete piles were 14-in. x 14-in. square and driven to depths on the order of 82-ft. The timber piles were tapered, with a 7.5-in. tip diameter and 14-in butt diameter, and driven to depths on the order of 63-ft. (Note: An average diameter of 10.75-in. was used in the back-calculation of measured unit side resistance for these tapered timber piles, which is described later in the paper.)

Each concrete and timber test pile was driven using a Vulcan 06 air hammer, and the associated driving records are provided in Fig. 5. Load-displacement curves for the static compression load tests on the driven concrete and timber piles are provided in Fig. 6. Load-displacement data for the static uplift tests are provided in Fig. 7. The maximum test loads for these piles are summarized in Table 2.

Measured Versus Predicted Driven Pile Capacity

The first methodology to predict the unit side resistance (f_p) of piles driven in clay soil, known as the "alpha method," was proposed by Tomlinson (1957) and can be expressed as follows:

$$f_p = \alpha \, s_u \tag{3}$$

where s_u = mean undrained shear strength along the length of the pile and α = an empirical coefficient, which is a function of s_u. It should be noted that α decreases as s_u increases. The Tomlinson (1957) database included measurements of s_u obtained from lower-quality strength testing, such as the UC or unconsolidated undrained (UU) triaxial test. For the range of mean s_u(UC) values encountered at the subject site, a corresponding $\alpha = 0.55$ would be appropriate (Tomlinson, 1957).

Using the mean laboratory values of s_u(UC) for the site, back-calculated (measured) values of α(UC) were determined for the driven steel pipe, concrete, and timber piles, as provided in Tables 1 and 2. For the load tests which were conducted to geotechnical failure, measured values of α(UC) range from 0.62 to 0.77 (Tables 1 and 2). Using Eqn. 3 in conjunction with laboratory values of s_u(UC) and α= 0.55 (Tomlinson, 1957), corresponding ratios of measured-to-predicted unit side resistance (f_m/f_p) range from 1.13 to 1.40 for the piles that reached full geotechnical failure, as shown in Table 3. These data indicate that the use of the Tomlinson (1957) prediction methodology, in conjunction with laboratory measured values of s_u(UC), is somewhat conservative for this particular site.
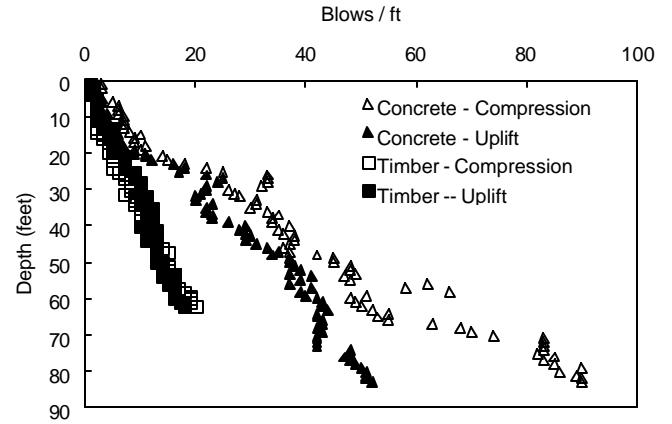

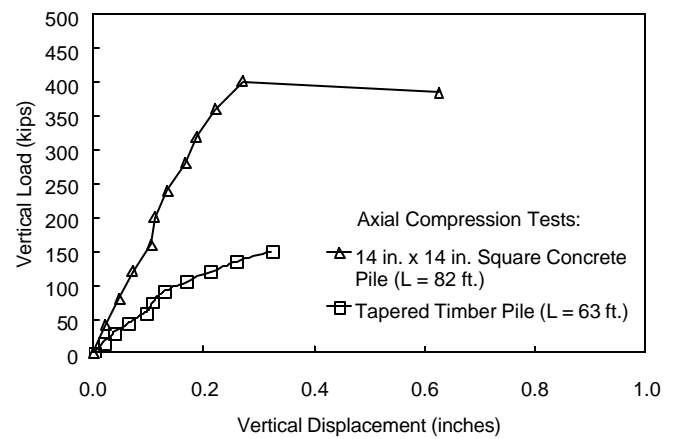Fig. 5. *Driving records for concrete and timber piles*

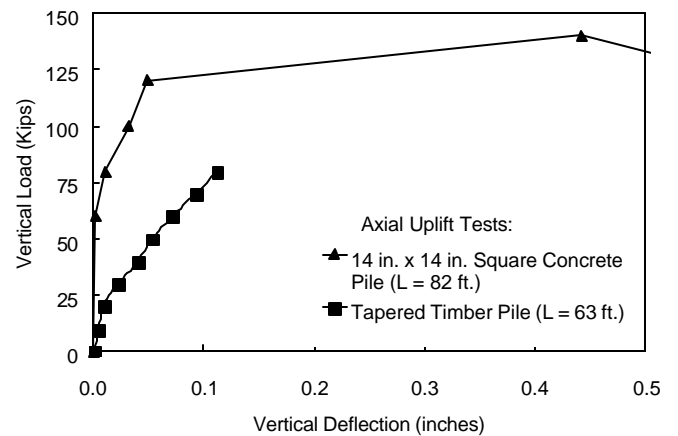Fig. 6. *Load-displacement curves for axial compression load tests on driven concrete and timber piles*

Fig. 7. *Load-displacement curves for axial uplift load tests on driven concrete and timber piles*

Values of unit side resistance can also be predicted from the results of the CPTU q_T data by converting the in situ data to equivalent values of direct simple shear (DSS) undrained shear strength using the following formula (Aas, et al., 1986):

$$s_u(DSS) = 0.0667 \, [q_T - \sigma_{vo}] \tag{4}$$

For the range of equivalent mean $s_u(DSS)$ values encountered at the subject site, as reported in Table 4, a corresponding $\alpha = 0.25$ would be most appropriate (Tomlinson, 1957). The use of Tomlinson's α factor with equivalent $s_u(DSS)$ data was selected simply because an alternate $\alpha(DSS)$ has not been developed to date to be used specifically for driven piles. The resulting values of predicted unit side resistance (f_p) using Eqns. 3 and 4 for the driven steel pipe, concrete, and timber piles are provided in Table 4. For the load tests which were conducted to geotechnical failure, corresponding ratios of measured-to-predicted unit side resistance (f_m/f_p) range from 1.26 to 1.54, indicating that the use of the Tomlinson (1957) α factor in conjunction with equivalent values of $s_u(DSS)$ inferred from the correlation with CPTU q_T, is somewhat more conservative compared to the use of the Tomlinson (1957) α factor in conjunction with laboratory measured values of $s_u(UC)$ for this particular site.

DRILLED SHAFT FOUNDATION FOR THE NEW BRADDOCK GATED DAM—BRADDOCK, PA

The U.S Army Corps of Engineers recently completed construction of the drilled shaft foundation for a replacement dam to improve the performance and serviceability of Lock and Dam No. 2 on the Monongahela River near Braddock, Pennsylvania. This new dam was constructed by floating hollow, modular dam segments to the site, submerging them onto the drilled shaft foundation, and subsequently filling the segments with concrete, grouting the underbase, and tremie grouting the dam-drilled shaft connections.

Rock-socketed drilled shafts were used to support the modular segments, and the design axial and lateral loads were several hundred kips each. To validate the design for the production shafts, an axial and lateral load testing program was conducted prior to construction. Details and critical findings of this load testing program are summarized in the following subsections.

Geotechnical Conditions

The base of the dam is at El. 683.7 ft., which is about 15 feet below the existing riverbed. The stratigraphy at the site consists of alluvium between Elevations 683.7 ft. and 668.0 ft., which is classified as a sandy gravel (GM) to silty sand with gravel (SM). Soft to medium hard clay shale and claystone starts at El. 668.0 ft. and extends to El. 658.0 ft. Medium hard to hard siltstone is encountered between Elevations 658.0 ft. and 626.0 ft. These stratigraphic layers

are shown schematically in Fig. 8 relative to the river normal pool elevation (718.7 ft).

Test Shaft Construction, Load Test Equipment and Instrumentation

A test location in the river was selected to encounter the weaker rock stratigraphy inferred from the subsurface exploration of the dam site. Two test shafts ("A" and "B") were constructed and load tested at the subject site. To provide sufficient space to accommodate the lateral load test equipment, the top of the test shafts were constructed to El. 690.0 ft. As shown in Fig. 8, the base of Test Shaft A was constructed to El. 653.0 ft. while the base of Test Shaft B was constructed to El. 643.0 ft. The diameter of the rock-socketed test shafts below El. 668.0 ft. are 60-inches (5-ft). However, the use of a 66-inch (5.5-ft) diameter steel casing through the alluvium layer resulted in a slightly wider shaft between Elevations 690.0 and 668.0 ft. Vertical reinforcement for each shaft consisted of twelve (12) #18 Grade 60 rebars with #8 rebar hoops with alternating lap splices and a minimum 4-inch clear spacing.

As the test location was in the river, conventional load testing was impractical. Therefore, the axial load testing was performed using Osterberg load cells. The load cell for Test Shaft A was 11.5-inches high, 21-inches in diameter, and was fitted with top and bottom steel plates, 34- and 52-inches in diameter, respectively, and each 2-inches thick. To provide the capability of applying higher loads, the Osterberg load cell assembly used for Test Shaft B consisted of three (3) 26-inch diameter load cells welded to top and bottom plates, each 56.75-inches in diameter and 2-inches thick. Two linear, variable vibrating-wire displacement transducers (LVWDTs) were set and attached to the top and bottom plates of the Osterberg load cell assembly in each shaft to measure the cell expansion/compression at two diametrically opposed locations. Telltales with LVWDTs were also installed to measure shaft compression with depth, as well as the movement of the top of each Osterberg cell.

The lateral load test was conducted by running a #20 Grade 80 bar between Test Shafts A and B at El. 684.7 ft., 1-ft above the pre-excavated river bottom. The lateral load was applied by a hydraulic jack at Test Shaft B, while readings of lateral load were obtained by a load cell placed on the #20 bar at Test Shaft A.

The vertical reinforcement in each shaft was fitted with weldable strain gauges; while additional strain gauges were embedded in the concrete. Also, a string of vibrating wire inclinometers was installed in each shaft to develop lateral deflection profiles.

Axial Load Test Results

Prior to the lateral load test program, Stage I axial testing was performed on Test Shaft A without causing significant

Table 1. Back-calculated values of unit side resistance (f_m) and α(UC) from static compression load tests on pipe piles

Pipe Pile No.	Measured Comp. Capacity (kips)	Back-calculated (Measured) Values	
		f_m (psf)	$α^{(2)}$ (UC)
1	>200[1]	>1049[1]	>0.76[1]
2	163	855	0.62
3	181	950	0.69
4	200	1049	0.76
Mean	186	976	>0.71

(1)—Test terminated prior to geotechnical failure
(2)—Using mean laboratory measured s_u(UC) = 1375 psf

Table 2 Back-calculated values of unit side resistance (f_m) and α(UC) from static load tests on concrete and timber piles

Pile Type & Loading Mode	Measured Capacity (kips)	Back-calculated (Measured) Values	
		f_m (psf)	$α^{(1)}$ (UC)
Concrete (U)	140	NA[2]	NA[2]
Timber (U)	>80[3]	>452[3]	>0.47[3]
Concrete (C)	400	1045	0.77
Timber (C)	>150	>738	>0.54

(UC)—Unconfined Compression
(C)—Compression; (U)—Uplift
(1)—Using mean laboratory measured s_u(UC)
(2)—Failure mechanism inconclusive (splice yielding vs. geotechnical failure)
(3)—Test terminated prior to geotechnical failure

Table 3. Measured and predicted values of unit side resistance (f_m, f_p) for driven pipe, concrete, and timber piles using laboratory s_u(UC) data

Pile Type & Load Mode	f_m (psf)	Predicted Values			
		$s_u^{(1)}$ (UC) (psf)	$α^{(2)}$	$f_p^{(3)}$ (psf)	f_m/f_p
Pipe 1 (C)	>1049[5]	1375	0.55	756	>1.38[5]
Pipe 2 (C)	855	1375	0.55	756	1.13
Pipe 3 (C)	950	1375	0.55	756	1.26
Pipe 4 (C)	1049	1375	0.55	756	1.39
Conc. (U)	NA[4]	1360	0.55	NA[4]	NA[4]
Timb. (U)	>452[5]	1340	0.55	737	>0.61[5]
Conc. (C)	1045	1360	0.55	748	1.40
Timb. (C)	>738[5]	1340	0.55	737	>1.00[5]

(UC)—unconfined compression test
(C)—Compression; (U)— Uplift
(1)—Laboratory measured values
(2)—Tomlinson (1957)
(3)—$f_p = α\, s_u$(UC)
(4)—Failure mechanism inconclusive (splice yielding vs. geotechnical failure)
(5)—Test terminated prior to geotechnical failure

Table 4. Measured and predicted values of unit side resistance (f_m, f_p) for driven pipe, concrete, and timber piles using s_u(DSS) data inferred from correlation with CPTU q_T

Pile Type & Load Mode	f_m (psf)	Predicted Values			
		$s_u^{(1)}$ (DSS) (psf)	$α^{(2)}$	$f_p^{(3)}$ (psf)	f_m/f_p
Pipe 1 (C)	>1049[5]	2725	0.25	681	>1.54[5]
Pipe 2 (C)	855	2725	0.25	681	1.26
Pipe 3 (C)	950	2725	0.25	681	1.40
Pipe 4 (C)	1049	2725	0.25	681	1.54
Conc. (U)	NA[4]	2958	0.25	NA[4]	NA[4]
Timb. (U)	>452[5]	2755	0.25	689	>0.66[5]
Conc. (C)	1045	2958	0.25	740	1.41
Timb. (C)	>738[5]	2755	0.25	689	>1.07[5]

(DSS)—direct simple shear
(C)—Compression; (U)— Uplift
(1)—As inferred from CPTU q_T (Aas, et al., 1986)
(2)—Tomlinson (1957)
(3)—$f_p = α\, s_u$(DSS)
(4)—Failure mechanism inconclusive (splice yielding vs. geotechnical failure)
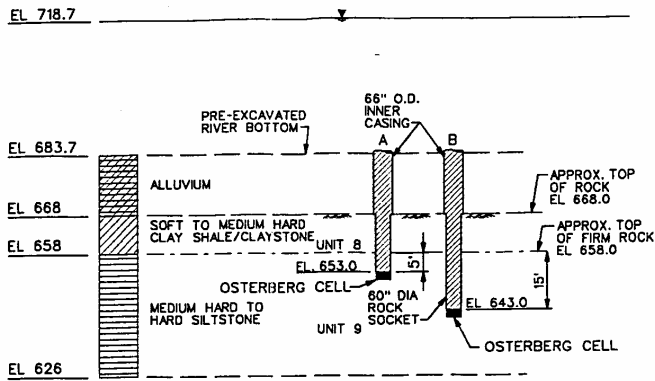(5)—Test terminated prior to geotechnical failure

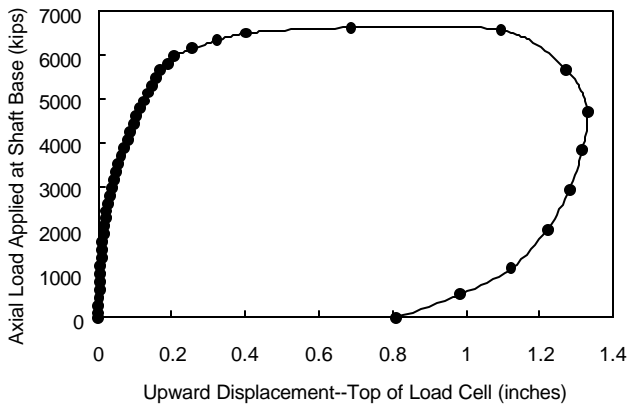Fig. 8. Soil and rock stratigraphy at Braddock Dam test site

Fig. 9. Base Load versus Upward Displacement of the Top of the Osterberg Load Cell, Test Shaft A, Stage II.

displacement prior to the lateral load testing program. Therefore, the Stage I axial test load was limited to 1478 kips, which corresponded to approximately half of the anticipated (estimated) ultimate side resistance. The test load was applied to the base of the shaft, resulting in upward (+) and downward (-) displacements of the top and bottom plates of the Osterberg cell of +0.016 inch and -0.03 inch, respectively. Accounting for the weight of the shaft, the mobilized side shear in the rock socket at the end of Stage I loading was approximately 5750 psf (40 psi).

After the lateral load test was conducted on Test Shaft A, Stage II axial testing was performed. A maximum axial load of 6620 kips was applied to the base of the shaft, resulting in upward and downward displacements of the top and bottom plates of the Osterberg cell of +0.69 inch and -0.10 inch, respectively. A plot of the upward displacement of the top of the Osterberg load cell as a function of load is provided in Fig. 9. The data clearly indicate that the ultimate side resistance was achieved. Accounting for the weight of the shaft, the measured ultimate unit side resistance in the rock socket at the end of Stage II loading was approximately 27,500 psf (190 psi). These results indicate that the measured ultimate unit side resistance of the rock socket was more than double the estimated ultimate unit side resistance.

The average measured unconfined compressive strength (q_u) of the claystone and siltstone was 844 psi; therefore, the ultimate measured side resistance of 190 psi is approximately equal to $0.23q_u$. Bond stress data reported by Horvath (1978) on rock-socketed drilled shafts indicate that for q_u less than 1000 psi, the ultimate rock-grout bond stress ranges from approximately $0.1 q_u$ to $0.2 q_u$. Also, for the design of small diameter grouted rock anchorages in hard shales, the PTI (1996) recommends ultimate bond stresses ranging from 120 to 200 psi. The data indicate that the measured ultimate unit side resistance for the load-tested rock socket of Test Shaft A either approximately equals or slightly exceeds the traditional published upper bound values of ultimate unit side resistance.

A more recent empirical study on drilled shaft side resistance in rock (Kulhawy and Phoon, 1993) resulted in the following mean relationship:

$$f_p = q_u \left[\frac{2}{\sqrt{q_u / 2p_a}} \right] \qquad (5)$$

where p_a = atmospheric pressure. In addition, Kulhawy and Phoon (1993) proposed a lower-bound to f_p equal to half of the mean value reported in Eqn 5. Use of this prediction methodology for q_u = 844 psi results in mean and lower-bound ultimate side resistances of $0.37 q_u$ and $0.19 q_u$, respectively. The measured value of $0.23 q_u$ is within these two values. Hence, the use of the mean relationship reported by Kulhawy and Phoon (1993) is unconservative relative to the value measured at the subject site. Therefore, unless a higher value of ultimate unit side resistance is verified by full-scale field testing, use of the lower-bound correlation for ultimate unit side resistance (e.g., 50% of the mean reported in Eqn. 5) proposed by Kulhawy and Phoon (1993) is recommended for preliminary design.

Considering the 52-inch diameter base plate for the Osterberg load cell in Test Shaft A, the maximum applied end bearing stress at the maximum load of 6620 kips was approximately 3117 psi, or 3.7 q_u. A recent evaluation by Kulhawy and Prakoso (1999) indicates that the ultimate unit tip resistance in rock (q_{ult}) can be estimated conservatively as:

$$q_{ult} \approx 0.9 q_u N_c \qquad (6)$$

where N_c = bearing capacity factor. Kulhawy and Prakoso (1999) reported a mean value of 4.34 for N_c, with a standard deviation of 2.13 and coefficient of variation of 0.49. Clearly, Eqn. 6 is consistent relative to the data collected for Test Shaft A.

Attempts were made to perform axial load tests on Test Shaft B. However, during the initial stages of the test it became apparent that the seating layer of grout below the bottom bearing plate of the Osterberg load cell assembly had insufficient strength to transmit the applied load to the base of the shaft. The average downward movement of the bottom

assembly plate exceeded -0.2 inch at a load of only 236 kips. This downward displacement continued until the test was terminated at a load of 500 kips.

Lateral Load Test Results

The lateral load test was performed by pulling the two test shafts toward each other using a hydraulic jack and a single #20 Grade 80 bar connected to each shaft at El. 684.7 ft., 1-ft. above the pre-excavated river bottom. The lateral load test was performed to a maximum lateral load of 350 kips.

The lateral load-displacement curves for the shafts, evaluated at the top of the alluvium layer (El. 683.7 ft.), are provided in Fig. 10. At the maximum test load of 350 kips, the corresponding lateral displacement of each shaft at the groundline (El. 683.7 ft.) was approximately 1.15 inches. However, at this same maximum test load, the lateral displacement of each shaft at the top of rock (El. 668.0 ft.) was less than 0.02 inch. The lateral displacement profile for the rock-socketed portion of the shaft exhibited only one point of curvature, and the lateral displacement at the base of each shaft was essentially zero.

On the basis of the lateral load test, LPILE v3.0 was used to simulate the lateral load-displacement behavior of the test shafts at the groundline and within the rock socket. The Reese (1997) method for weak rock was used to develop p-y curves for the soft to medium hard clay shale and sandstone.

The use of the soil and rock parameters reported in Table 5 resulted in predicted lateral shaft displacements at the groundline and within the rock socket which were similar to the measured values.

The production shafts were step-tapered from a 78-inch diameter, permanently cased section through the alluvium to a 72-inch diameter rock socket. Using the Reese (1997) method, the rock parameters listed in Table 5 were subsequently employed to develop p-y curves for these larger production shafts at the top and 6-ft into the layer of soft to medium hard clay shale and claystone (El. 668.0 and 662.0 ft). The resulting p-y curves for these 72-inch diameter production rock sockets are presented in Fig. 11.

Since the lateral load test was not performed to geotechnical failure of the rock socket, the ultimate lateral capacity of the rock is not known. However, the test shafts performed satisfactorily, considering the minimal lateral deflection of the socketed portion of the shaft under the applied design load.

SUMMARY

In this study, two case histories of deep foundations, including driven piles and drilled shafts, were addressed. The first case history provided an assessment of driven pile capacity in
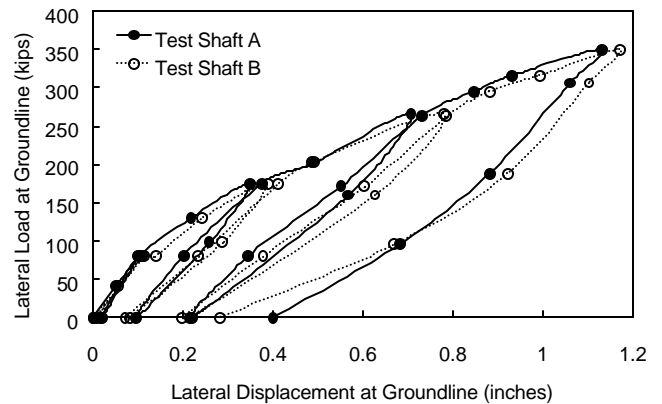

Fig.10. Lateral Load versus Lateral Groundline Displacement (El. 683.7 ft.), Test Shafts A & B.

Table 5. Soil and rock parameters developed from laboratory testing and test shaft results

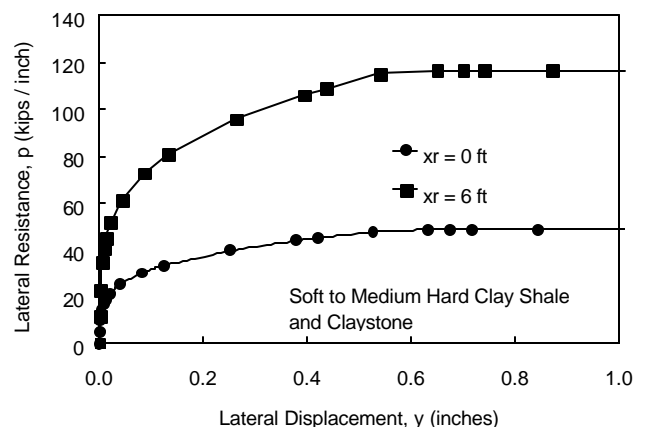| Subsurface Material	Parameter	Value
Alluvium	ϕ'	32°
	Subgrade modulus (k)	60 lb/in.
Claystone & Siltstone	q_u	844 psi
	RQD	30%
	ε_{50}	0.0005
	Subgrade modulus (k)	60,000 lb/in.
	Modulus Ratio	100 to 200
	Rock Mass Modulus Reduction Ratio	0.2 to 0.8

Fig. 11. Generated p-y curves at the surface and 6 ft into the soft to medium hard clay shale and claystone at the Braddock Dam test site

clayey soil. As part of the deep foundation material selection, steel pipe, concrete, and timber piles were driven at the site.

The data demonstrate that the traditional alpha method results in somewhat conservative predictions for the test piles if either laboratory values of undrained shear strength (s_u) obtained from the unconfined compression (UC) test or equivalent direct simple shear (DSS) values of s_u inferred from a correlation with the CPTU are used in conjunction with the original Tomlinson (1957) α factor.

The second case study involved an evaluation of capacity of drilled shafts in rock to support a concrete gated dam. Axial and lateral load tests were performed on test shafts embedded in granular alluvium and socketed into rock. The data demonstrate that while the predicted ultimate unit side resistance using more dated correlations or presumptive values was conservative relative to the measured value back-calculated from the axial load test, field verification should be employed to verify higher mean values of ultimate side resistance if determined by the more recent empirical relationship suggested by Kulhawy and Phoon (1993). The lateral load test indicated that the test shafts performed satisfactorily, considering the minimal lateral deflection of the socketed portion of the shaft under the applied load. In addition, the tests also suggested that a significant component of the lateral load resistance was derived from the alluvium soil above the rock.

ACKNOWLEDGEMENTS

REFERENCES

Aas, G., Lacasse, S., Lunne, T., and Hoeg, K. [1986]. "Use of In-Situ Tests for Foundation Design on Clay," *Use of In-Situ Tests in Geotechnical Engineering, ASCE GSP No. 6*, pp. 1-30.

Bjerrum, L. [1972]. "Embankments on Soft Ground," *Proc. Conf. on Performance of Earth and Earth-Supported Structures*, ASCE, Vol. 2, pp. 1-54.

Chen, Y.-J., and F.H. Kulhawy [1994]. "Case History Evaluation of the Behavior of Drilled Shafts Under Axial and Lateral Loading," *Report TR-104601,* Electric Power Research Institute, Palo Alto.

Horvath, R.G. [1978]. "Field Load Test Data on Concrete-to-Rock Bond Strength for Drilled Pier Foundations," *Report 78-07*, Department of Civil Engineering, University of Toronto, Ontario, Canada, 97 p.

Kulhawy, F.H., B. Birgisson, and M.D. Grigoriu [1992]. "Transformation Models for In-Situ Tests," *Report EL-5507(4),* Electric Power Research Institute, Palo Alto.

Kulhawy, F.H. and K.-K. Phoon [1993]. "Drilled Shaft Side Resistance in Clay Soil to Rock," *Design and Performance of Deep Foundations: Piles and Piers in Soil and Rock, ASCE GSP No. 38*, pp. 172-183.

Kulhawy, F.H. and W.A. Prakoso [1999]. Discussion of "End Bearing Capacity of Drilled Shafts in Rock," *J. Geotech Eng*, ASCE, Vol. 125, No. 12, pp. 1106-1109.

Ladd, C.C. and R. Foott [1974]. "New Design Procedure for Stability of Soft Clays," *J Geotech Eng*, ASCE, Vol. 100, No. 7, pp. 763-786.

PTI [1996]. *"Recommendations for Prestressed Rock and Soil Anchors,"* Post-Tensioning Institute, Phoenix, Arizona, 70 p.

Reese, L.C. [1997]. "Analysis of Laterally Loaded Piles in Weak Rock," *J Geotech Eng*, ASCE, Vol. 123, Vol. 11, pp. 1010-1017.

Tomlinson, M.J. [1957]. "The Adhesion of Piles Driven in Clay," *Proc. 4th Intern. Conf. Soil Mech.*, London, Vol. 2, pp. 66-71.